A Very Low-Noise Single-Sideband Receiver for 200–260 GHz

NEAL R. ERICKSON, MEMBER, IEEE

Abstract—**A cryogenic Schottky diode mixer receiver has been built for the 230-GHz region with true single-sideband operation and a receiver noise temperature as low as 330 K. Local oscillator power is provided by a frequency tripler, with LO injection and sideband filtering accomplished through quasi-optical interferometers. The image sideband is terminated in a cryogenic load with an effective temperature of 33 K. The IF bandwidth is 600 MHz with nearly flat noise, and the RF band is nearly flat over 50 GHz using backshort tuning of the mixer.**

I. Introduction

SCHOTTKY DIODE mixers for the 230-GHz region have shown a rapid improvement over the past five years as interest in this spectral region has increased. While local oscillator sources have long been regarded as a major limitation, the development of high-efficiency frequency triplers [1], [2] has solved this problem, making practical receivers for this band possible. At the same time, mixers and associated components have evolved to approach the performance attainable at lower frequencies. The best previously reported cryogenic mixer receiver for this frequency [3] operated double sideband with a DSB noise temperature of 235 K. Since this mixer is fixed tuned, its useful bandwidth is limited to 30 GHz.

This paper reports on a true single-sideband receiver covering 200–260 GHz which achieves substantially lower noise, and at the same time has a useful IF bandwidth of over 600 MHz. This receiver has required major advances in several critical elements, and a rather novel optical design.

The receiver consists of a single wide-band backshort tunable mixer and 1.1–1.7-GHz FET IF amplifier, both operating at ~ 20 K inside a vacuum dewar. Local oscillator power is provided by a frequency tripler. Optical elements are used to separate the signal and image bands in the mixer response, to inject the LO into the mixer, and to direct the image response to a 20-K termination within the vacuum dewar. Suppression of the image response is essential for well-calibrated observations of spectral line sources in radio astronomical observations. For the case of a cryogenic image termination, an additional advantage is that this termination adds very little to the total system noise, while double-sideband receivers pick up an additional and sometimes substantial noise contribution from the effective image temperature.

Manuscript received March 1, 1985; revised June 6, 1985. This work was supported in part by the National Science Foundation, under Grant AST-82-12252.

The author is with the Five College Radio Astronomy Observatory, University of Massachusetts, Amherst, MA 01003.

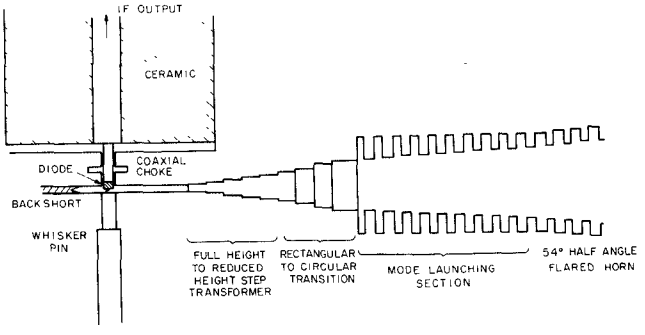

Fig. 1. Cross section of mixer and throat section of feed horn.

II. Mixer

The mixer design is central to the receiver performance. The mixer uses ~1/3 height waveguide of dimensions 0.16×0.91 mm with an eight-section step transformer to a corrugated horn, and is shown in cross section in Fig. 1. The step transformer is designed to avoid spurious resonances and to maintain a low VSWR over the full frequency range. A step in width is made between the rectangular to circular transition and the actual mixer waveguide, since 0.91-mm width seemed necessary to allow the mixer to reach the upper edge of the 200–260-GHz band, while the existing rectangular to circular step transition [4] was designed for rectangular waveguide 0.98 mm wide in order to cover the same band.

The IF filter choke is a very simple air dielectric radial mode choke used in several other comparable frequency mixers [7]. It was chosen because it is easily fabricated with good control of critical parameters, and has a center pin of constant diameter for maximum rigidity, allowing the diode chip to be soldered on and carefully ground down *in situ* to the exact diameter of this pin. This choke has no stopband at second harmonic frequencies. The diode chip was fabricated by R. Mattauch (Univ. of Virginia) and is from batch 1H2. The anodes are 1 μm diameter with a zero-bias capacitance of 1.8 fF and a room-temperature series resistance of 15 Ω. The epitaxial layer doping is 4×10^{-16} cm^{-3} with a thickness of 0.17 μm. These diodes show a steepening of the logarithmic slope of the I–V curve by a factor of 3.3 upon cooling to 20 K, and a comparable reduction in mixer noise. At the same time, the

0018-9480/85/1100-1179$01.00 ©1985 IEEE

dc series resistance increases to 19 Ω. This yields an extremely high 1/RC cutoff frequency of 4.7 THz, while the very low capacitance allows the diode impedance to more readily match that of the waveguide, without resorting to the extremely reduced-height guide. This means that the waveguide is more easily fabricated, that a contacting backshort can operate more reproducibly, and that waveguide losses are reduced.

Corrugated horns present fabrication problems at these frequencies because most design criteria require many very thin corrugations per wavelength [6] and a mode launching section with rather deep, narrow grooves. However, other authors have suggested that fewer grooves are needed if less stringent performance standards are set [5]. This horn was designed around a more relaxed set of criteria, and has a corrugation period of 0.41 mm, or ~3 grooves per wavelength, with rather thick walls. Most grooves are 0.31 mm deep, or $\sim\lambda/4$ at midband, while in the mode launching section, grooves start at 0.52 mm deep ($\lambda/2$ at the high end of the band) and taper in depth over 10 grooves to the $\lambda/4$ depth. The horn tapers at 5.4° half angle to an aperture of 9.0 mm, and behaves as a constant aperture over the band 200–290 GHz. The complete length of the horn is 44 mm. To test this design, a 2.4-times scaled prototype was built in the WR-10 band, including the rectangular to circular transition, and was compared to a rectangular horn for insertion loss by using both as feeds for a low-noise radiometer. No significant difference was found between the losses of the two horns over the full scaled operating band. Beam patterns were also measured for this model and agreed well with the expected patterns over the band. This horn is coupled to incoming radiation through a 0.5-mm teflon dewar window tilted at Brewster's angle (55°) for zero reflection loss independent of frequency. The horn is very close to this window to minimize the window area and to allow the next mirror to be placed sufficiently close to the horn.

The entire mixer waveguide and feed horn are electroformed as a single unit with a minimum length of reduced-height guide between the horn and mixer diode. This waveguide was made using an aluminum mandrel, gold-plated, and then copper-plated up to the needed thickness. The inside gold plating is probably not optimum for such a mixer because tests of typical gold-plated waveguide at room temperature show losses ~1.2 times that of machined OFHC copper, and also because the conductivity of gold increases much less at cryogenic temperatures than that of copper. However, the short length of waveguide involved has an expected loss of ~5 percent so is not very important in any case. The IF choke center conductor is supported in a ceramic (Macor) [16] ring tapered and pressed into a wafer bolted to that containing the waveguide, with the choke center pin gold-plated and pressed into the Macor ring. This assembly can be made extremely rugged and has survived many thermal cycles with no diode failures.

One-micron diode anodes present greater difficulty in contacting than do larger anodes, but have shown no greater contact instability upon thermal cycling. However, for any diode, the rather short whiskers (~0.2 mm) needed for this mixer tend to produce excessive contact pressure on the diode, if 12-μm-diam Ph-bronze wire is used. This excessive pressure produces little effect at room temperature, but, upon cooling, the *IV* curve may be significantly degraded (less steep slope), probably due to stress-induced microcracking of the epitaxial layer. This is accompanied by an increase in noise. To avoid this problem, whisker wires are thinned to 6 μm diam using the same solution used to sharpen them. Contact whiskers must be made ~20 percent shorter to compensate for the increased inductance of this thinner wire. Whiskers are gold-plated, soldered onto the final whisker pin, and then bent to shape. The typical overall length for a 6-μm-diam wire is 0.2 to 0.25 mm.

Whisker pins are 0.50-mm BeCu turned down to 0.32 mm diam where they pass through the waveguide wall. These pins are pressed through a close fitting hole in the block adjacent to the waveguide block. It has been found that up to 10–15 μm of gold can be plated on the BeCu pins to improve the fit. Greater amounts will quickly flake off and would require an intermediate binding layer to improve the adhesion.

While an effort was made to maintain tolerances of 5 μm throughout the fabrication of the mixer, there are some perceptible irregularities in the throat of the horn, where errors may reach ~10 μm and where machining burrs may still be present. However, two mixers of this design have shown nearly identical performance, so fabrication is not an apparent limitation.

The mixer backshort is a contacting design made from a Ph-bronze shim with a simple V groove in the end. This groove has an opening angle of 35° and extends across the width of the short. This shim is heavily gold-plated and the V spread apart with a sharp blade, and then forced into the flared open end of the guide. This type of short produces excellent performance for a large number of tuning cycles, but eventually tends to become erratic if it is tuned too much. A noncontacting type of short might possibly be feasible but has not been attempted, and would be considerably more fragile. Fixed-tuned backshorts have been advocated to eliminate these problems [3], but this mixer design achieves wider bandwidth and lower noise than a fixed-tuned mixer. Backshort wear is not a real problem in this mixer since all data presented here was measured after five months of use on the FCRAO 14-m antenna with no backshort alterations, and shows no deterioration in performance over previous measurements.

III. IF Matching Circuit

For minimum IF passband ripple and lowest conversion loss, an effective IF matching circuit is needed. This is particularly true when using a very low-capacitance diode which raises the overall mixer impedance level and results in an IF impedance of ~400 Ω at room temperature, and probably a similar value when cold. The approximate effect of the RF choke and ceramic supporting ring is to

add a parallel capacitance of 0.93 pF. This can be matched with a low wide-band VSWR to 50 Ω by simply adding a 10-nH lumped inductor between the IF pin and the IF stripline. The resulting IF return loss was measured at room temperature and is 10 dB at the edges of a 500-MHz band and exceeds 15 dB at band center. A somewhat flatter match could be accomplished by adding a shorted $\lambda/4$ stub but the improvement is only marginal, and adds some additional loss as well. The matching circuit and a bias-T/dc block are incorporated on stripline in a small cutout box included as part of the mixer block.

IV. IF Amplifier

The cryogenic IF amplifier is a three-stage FET design similar to that described by Weinreb *et al.* [8]. Electrically it is equivalent, but a duroid substrate with microstrip interconnections was used to simplify parts mounting. An input matching transformer and stub were used to increase the bandwidth as in the original design, but this model uses 0.63-mm alumina as the substrate with the alumina ground plane soldered down using pure indium. This has the advantage of producing an amplifier which can be tuned up entirely at room temperature, with little or no retuning needed for 20-K operation. The bandwidth is 600 MHz (1100–1700 MHz) with an average noise temperature at 77-K ambient of ~15 K. This should decrease to ⩽10-K at 20-K ambient but was not measured due to the extra complexity of 20-K measurements. The gain at 77 K is 29–32 dB across the full band. Input return loss is >15 dB (VSWR <1.5/1). There is little evidence for FET self-heating due to the relatively poor thermal conductivity of the duroid board since the noise temperature is quite insensitive to drain current, at least at 77 K.

V. Optics

Much of the superior performance of this receiver can be attributed to an unconventional optical design. A design goal was true SSB operation, and since it is difficult to tune a mixer for flat SSB response without a very high IF, it is essential to use an input filter and image load. In order to minimize the additive noise due to the temperature of the image termination, this termination must be made as cold and as well matched as possible. For lowest loss, the input filtering must be done optically. Because the optics are somewhat large and massive, attempting to cool them would require a much larger refrigerator than needed otherwise. Since optics losses can be kept very low, a room-temperature design seemed more practical.

Optical elements need to serve the dual functions of LO injection and signal/image separation. No single optical element can perform these simultaneously so it is necessary to cascade filter elements. One of the simplest, as well as the lowest loss, optical filters available is the two-beam interferometer known as the Martin–Puplett interferometer (MPI) as shown in Fig. 3. However, this device has a

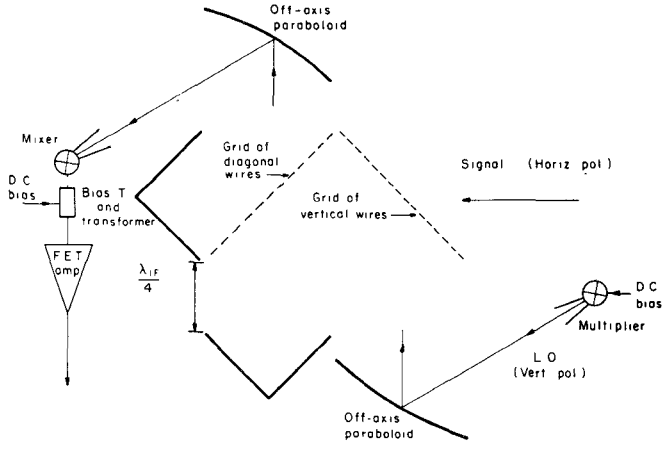

Fig. 2. Schematic diagram of Martin–Puplett interferometer. Wires of grid 1 are at 45° with respect to the incoming polarization, wires of grid 2 are aligned perpendicular to the incident signal beam.

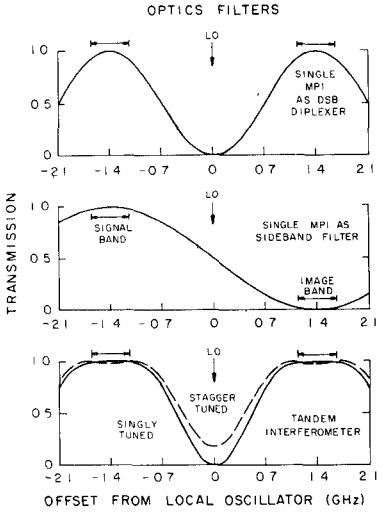

Fig. 3. Transmission versus frequency of various configurations of Martin–Puplett interferometers (MPI's). (a) Single MPI used as a LO signal diplexer in a DSB receiver. (b) Single MPI used as a sideband filter in a SSB receiver. (c) Tandem MPI used as LO filter and LO image sideband diplexer.

sinusoidal passband

$$T = 1/2\left(1 + \sin\frac{2\pi d}{\lambda}\right)$$

which is not optimal where wide bandwidth is needed.

One design requirement of this system was an IF bandwidth of over 500 MHz with little variation in noise. A previous receiver [7] used a single MPI in a DSB receiver by placing the LO, signal, and image bands within the passband as shown in Fig. 3(a). This works well over a narrow band, but in the case of a noisy LO source, the noise rises rapidly as the IF is tuned away from the band center. As a case in point, if the LO noise is only 300 K, as would be the case with a room-temperature attenuator in the LO path at an IF offset of 250 MHz from a 1400-MHz center frequency, the net signal and image transmission is 0.92, causing an additive noise temperature of $0.08 \times 300\ \text{K} = 24\ \text{K}$, as well as a signal reduction. Typical sources produce significantly greater noise than this so it is

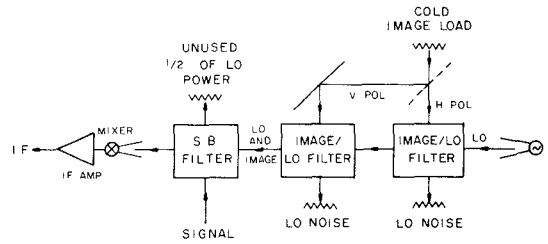

Fig. 4. Block diagram of 230-GHz receiver.

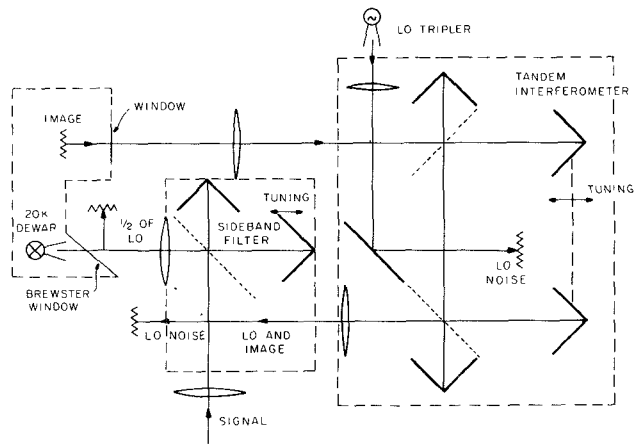

Fig. 5. Schematic diagram of optical path in 230-GHz receiver (lenses are used to represent mirrors). Vertical wire grids are shown as dotted lines, diagonal grids are shown as dashed lines.

essential to provide a better means of LO filtering, as well as a lower signal loss over the band. In order to minimize the receiver noise, the signal path should have the lowest optical loss, while the image and LO paths are less critical.

Therefore, an unconventional approach was taken. The LO injection interferometer as used in the DSB receiver was retained, but its path difference was decreased by a factor of 2, so that it becomes a sideband filter with a passband as shown in Fig. 3(b). Now the transmission is quite flat over a 500-MHz band with the minimum transmission being 0.98. Similarly, the image band is well rejected. The consequence of this is that the LO falls at point of 50-percent transmission and can be coupled in through the image arm.

A second interferometer follows in the image arm to separate the LO from the image. This interferometer has twice the path difference to allow optimum LO and image transmission. However, due to the bandwidth limitation mentioned before, this provides inadequate LO noise filtering as well as a poor wide-band image termination. This problem can be overcome by following the first image/LO separation interferometer with a second tuned in tandem. This is shown in the receiver block diagram of Fig. 4. This greatly flattens the passband, but requires two image ports, as well as double tuning. However, by a careful geometrical layout of the two, they can be made easily tandem tuned with only a single image port. This is shown in the receiver schematic in Fig. 5, where focusing mirrors are represented by lenses. The two image port inputs are in opposite polarizations and are combined on the input grid of the first filter to form a mixed polarization image input. The overall transmission of this tandem interferometer is shown in Fig. 3(c). The bandwidth with <1-percent increase in loss is 41 percent of the IF center frequency, or 574 MHz in this case. The polarization makeup of this image input depends upon frequency, changing from linear at band center, to up to an 8-percent horizontal component at the band edge. This introduces one additional constraint for the image termination, which is that it must work well in both polarizations.

This type of filter forms a superior alternative to a Fabry–Perot interferometer where a wide flat passband is needed, with low LO loss. It has a further advantage of a very wide tunable band since the wire grids behave as nearly ideal polarizers over several octaves. A Fabry–Perot would require ~ 90-percent reflectance mirrors to operate with comparable noise rejection, and, as a result, the LO loss would be appreciable and the tuning rather critical. One disadvantage of the present version is that the output is composed of two delayed Gaussians, which in this case have a rather low mode overlap, and thus cannot be treated as the same mode. However, the image termination is designed to accept both modes so this is not a problem. In other applications, this difficulty could be overcome by delaying one of the beams to equalize the paths and thus produce a perfect overlap.

Should an even wider passband be needed, the two interferometers could be stagger tuned, although this would result in a greater LO loss. As an example, if a peak theoretical LO transmission of 0.82 is acceptable, the two interferometers can be offset by 1/5 of a period, to yield a transmission bandwidth of 58 percent of the center frequency with a maximum loss of 1 percent. This corresponds to 812 MHz at a 1400-MHz center frequency.

In order to realize the low loss inherent in optical devices, it is essential to minimize diffraction loss and mode conversion. The scalar feed produces a beam which closely approximates a Gaussian profile with w_0 of 3 mm at all frequencies. For a Gaussian beam [11], [15], the intensity varies as

$$I(r,z) = e^{-2r^2/w^2} \quad \text{where} \quad w(z) = w_0\left(1+\left(\frac{\lambda z}{\pi w_0^2}\right)^2\right)^{1/2}$$

and z is the distance from a beam waist in the system. Assuming the feedhorn launches a 100-percent Gaussian beam, a minimum aperture size of 3.5 w is needed to reduce diffraction loss at a single aperture to 0.5 percent, and to minimize the contribution of room-temperature losses to the total system noise. Since several limiting apertures are involved, and because a scalar horn launches a mode in which only 98 percent of the power is in the Gaussian mode, it is desirable to allow somewhat greater clearance where possible, 4 w being the goal of this design. In this particular receiver, space constraints prevented using an optics clear diameter of more than 51 mm except at a few places where extra space was available. There is also a requirement in dual-beam interferometers that the mode overlap when the beams recombine be close to unity [10], and this establishes a minimum beam-waist size within the

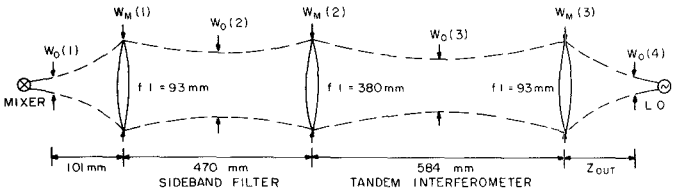

Fig. 6. Unfolded optical path between the tripler and mixer showing positions of focusing mirrors (represented as lenses here) and beam waists.

TABLE I
BEAM SIZE WITHIN RECEIVER OPTICS

f (GHz)	$w_0(1)$	$w_0(2)$	$w_0(3)$	$w_0(4)$ (all in mm)	$w_m(1)$	$w_m(2)$	$w_m(3)$	z_{out}
200	3.0	13.6	12.1	3.5	16.4	15.4	14.9	10.4
240	3.0	11.6	12.1	3.0	13.7	14.4	14.2	10.1
280	3.0	10.1	12.1	2.5	11.9	13.7	13.7	9.9

interferometer. The net transmission is given by

$$T=\frac{1}{4}\left[1+\left(1+\left(\frac{\lambda\Delta}{2\pi w_0^2}\right)^2\right)^{-1/2}\right]^2$$

and for $T>0.99$, requires $2\pi w_0^2/\lambda\Delta > 6.7$, where Δ is the path difference between the two arms. This in turn requires $w_0 > 8.5$ mm in the SB filter and $w_0 > 12$ mm in the tandem interferometer, and these sizes were designed into these optics.

One intermediate focusing mirror was found necessary in this design, and could conveniently be included as a 90° off-axis folding mirror. A second focusing mirror between the right-hand pair of interferometers would have allowed a somewhat more optimum design, but could not be included in a reasonable position except as a lens, which would introduce more loss than it would prevent. In fact, the final interferometer can have a significant loss with little effect since it serves only to prefilter the LO (LO loss is not too critical) and to terminate at most 8 percent of the image which leaks through the first filter. The unfolded optical path is shown in Fig. 6 and the various beam parameters are summarized in Table I. As is seen from this table, the requirement of 3.5-w clearance is maintained at all points in this beam for a clear diameter of 51 mm except for mirrors 1 and 2 at 200 GHz. Mirror 1 is actually 57 mm in diameter and so fulfills this, but mirror 2 is not, and increases the loss to ~1.5 percent.

To minimize the number of different mirrors needed, mixer, LO, and image port mirrors are identical 60° off-axis ellipsoids, machined using a special technique on a conventional milling machine [9]. Off-axis mirrors are inconvenient to work with, so all mirrors are followed by a flat to produce an inline offset optics path. A 60° off-axis angle was chosen as a compromise between the ideal of on-axis optics, and the realities of needed clearances. While mirror 2 is theoretically an ellipse, it is a fairly flat mirror, and an off-axis parabola of equivalent focal length was substituted since it was available, and, in this case of long focal length, differred only slightly from the needed ellipse (in general this is not true).

All beam splitters are free-standing polarizing grids of 25-μm gold-plated tungsten wires, spaced by 85 μm. The spacing varies by ~ 40 μm, due to irregularities in the wire winding frame, but this seems to cause no observable problems. Three grids have wires oriented at 35.26° (which becomes 45° in projection for a 45° beamsplitter) while, for all other grids, the wires are oriented along the short distance across the holding frame. A final grid is placed across the front of the Brewster window to the mixer port of the dewar to eliminate the 50 percent of the LO power which reaches this port in the wrong polarization. If not rejected, this power can produce a high VSWR on the tripler output and cause LO power instabilities.

It is difficult to deduce the actual loss of the optics in this receiver because the mixer cannot be used without them, and any single-frequency measurement using feedhorns is certain to be plagued by standing-wave problems at the level of accuracy needed. However, we can compare the sideband filter optics to a previous set which were identical except for having a larger beam size internally. With a clearance of only 3 w, the loss in this interferometer alone was only 5 percent higher than in the new version with 3.6-w clearance. (This is inferred from the change in receiver temperature using the identical mixer). Thus, it is unlikely that the diffraction losses in this new device exceed 2–3 percent and resistive losses in the wire grids and mirrors are likely not to exceed 1 percent, based on considerable experience with such elements.

A particular problem with this type of sideband filter is that for a mixer with equal sideband gains, no simple indication of correct tuning for SSB operation is available. The only methods available are either to optimize coupling to a strong signal source at the correct frequency, or as a more practical means, to determine the true zero path difference setting, through mechanical measurement of LO power peaks and nulls at various frequencies, and to offset from this point to the calculated SSB setting through an accurate displacement transducer. For laboratory tests, a simple method to tune up when the exact LO frequency is not known is to find the LO transmission peak nearest the desired path for SSB operation, and to then offset by $\pm\lambda/8$ for SSB operation. Increasing the path by $\lambda/8$ produces USB operation, while decreasing it produces LSB. In astronomical observations, the sideband ratio was found to be >19 dB through observations of the strong CO line at 230 GHz.

Losses in the tandem interferometer can be measured more directly by measuring the SSB receiver temperature at the signal port and at the image port in front of the dewar window. This shows a small increase in T_R, after correction for the higher termination temperature of the signal port. Assuming equal sideband gains, which can be verified through measurement, this increase in T_R must be due to optics losses, and these are found to be ~ 3 percent.

This loss is not too important, and only results in an increase in the effective image termination temperature from 33 K at the dewar window to 42 K at the output of the tandem interferometer. Peak LO noise rejection of this filter is measured to be 40 dB, and the rejection is > 20 dB over a 600-MHz bandwidth, in good agreement with theory.

VI. Off-Axis Reflective Optics

For applications at frequencies above 100 GHz, most dielectrics become to lossy to be suitable for lenses. The few common exceptions are polyethylene, teflon, crystalline quartz, and TPX. The surface reflectivity of all these materials is high enough to require some compensation. Matching grooves are difficult to machine in curved surfaces, and at λ (1.3 mm) become quite small as well. While crystal quartz can be readily matched with a layer of polyethylene, it is a relatively expensive material and is difficult to grind, and in any case the matching coating becomes frequency dependent.

An attractive alternative is to use reflective optics sufficiently far off-axis to allow clearance for the input and output beams. These surfaces may be readily machined using computer-controlled machines or using analog techniques. However, reflective optics are somewhat more difficult to design and use for several reasons.

One problem is due to geometrical projection effects. In the case of nearly parabolic reflectors used far off-axis, an initially uniform beam becomes weighted toward the axial point after reflection simply because one side of the beam must travel farther than the other before reflection. This produces a distortion which becomes worse as the reflector is used farther off its axis, particularly if the included angle of the beam is large. A second effect occurs because at long wavelengths diffracting beams behave in nongeometrical ways, and all optics tend to be within the near-field of the focal points of the system. These effects include a phase velocity which is greater than c, and a curvature of wavefronts which is entirely different than in the geometrical case [15].

Other effects occur because an amplitude distribution changes shape as it propagates within the near-field region. A particular simplification occurs if a Gaussian mode is used. This distribution retains its shape within the near-field region since it is a normal mode of the system. Thus, it may be treated in a particularly simple manner. Since a corrugated feed horn launches a mode which is 98-percent Gaussian, it is convenient to design optics around an entirely Gaussian distribution and to plan on a complete loss for the 2 percent higher mode content of the beam. These considerations are applied to the ellipsoidal mirror used to focus the input beam into the mixer as follows.

For consideration of geometrical weighting effects, this mirror may be regarded as paraboloidal since its figure is very similar. A geometrical Gaussian beam of width 16° between $1/e^2$ power points, reflecting at 60° off-axis from a parabola, is distorted by this reflection in such a way that the direction of the maximum intensity is displaced by 0.2° toward the axis. However, the resultant beam, while slightly asymmetric, has an overlap integral with a Gaussian of > 99.9 percent, and is broadened by only 1 percent relative to the perpendicular plane.

Phase errors due to diffraction were calculated for this beam at 230 GHz for a waist radius of 0.3 cm and the equivalent waist to mirror center spacing of 10 cm. In this case, the input beam phase differs by up to 0.1 λ from a simple geometrical spherical wave, but the phase error is mostly quadratic and may be accounted for by a small focus shift. The residual error is $\sim \lambda/40$. The output beam wavefront radius of curvature is sufficiently large that while the mirror is well within the near-field region, the curvature errors are $\leqslant \lambda/40$. Variations in phase velocity across the mirror, for both input and output beams, produce $\sim 4°$ of phase error. Thus, this mirror behaves nearly ideally for a single-mode beam, and is far superior to a lens.

VII. Frequency Tripler

The lack of any convenient fundamental local oscillator sources in the 1-mm-wavelength region has made the development of frequency multipliers essential to the use of this spectral region. Recent improvements in Schottky varactor diode technology have made it possible to realize high-efficiency multipliers for these frequencies. For this receiver, a simple wide-band tripler [2] has been constructed covering the 195–255-GHz range having a peak conversion efficiency of 12 percent, and a second scaled device for 250–300 GHz has been used to extend measurements to 300 GHz.

Circuit requirements for a tripler are a means of conjugate impedance matching to the varactor at the input and output frequencies, and a resonant reactive termination at the second harmonic to enhance the tripling efficiency. Also needed is a means of biasing the diode with dc without loss of efficiency. The input and output match is made somewhat difficult because the varactor impedance is largely capacitive with a relatively small resistive component. From model and theoretical studies, the appropriate circuit model for the pumped varactor in an optimized circuit is found to be a capacitor of value 0.3–0.4 $C_j(0)$ in series with a resistor of 25–50 Ω.

The varactor diode used in this work is U.Va.-type 5M5 having a zero-bias capacitance of 15 fF and series resistance of 9 Ω. This device is mounted in the half-height WR-3 output waveguide (chosen to be cutoff to the second harmonic) as shown in Fig. 7, with input power coupled through a five-section, 50-Ω coaxial low-pass filter. Input power to the tripler is supplied through WR-12 waveguide tapering down to 1/5 height ($Z_g \sim 100$ Ω). Power is then post coupled to the coaxial choke, with dc bias provided through a radial line filter in the opposite wall of the input guide.

Impedance matching at the input is greatly aided by a novel coaxial resonator using a reduced-diameter section on the whisker pin. This coaxial line is $\lambda/2$ long at the output frequency and so appears as a short circuit. At

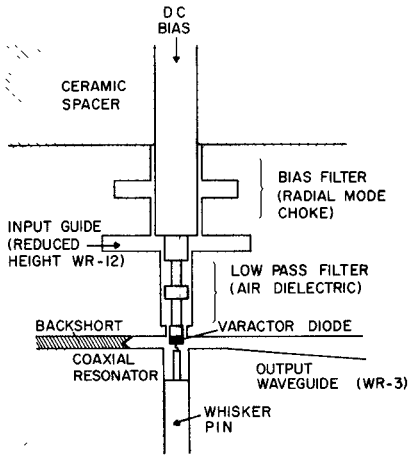

Fig. 7. Cross section through frequency tripler for 195–255 GHz.

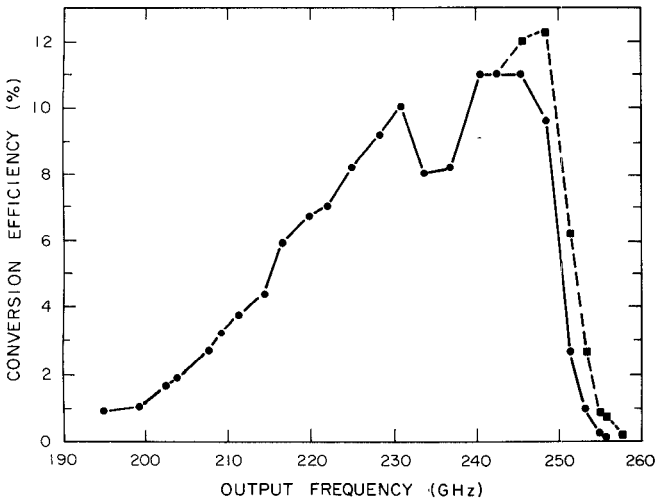

Fig. 8. Conversion efficiency versus frequency for frequency tripler. The solid curve is for an input power of 15 mW, while the dotted curve at the highest frequencies is for an input power of 30 to 60 mW.

midband for the input frequency, it is $\lambda/6$ long and appears inductive, with a reactance of $1.7jZ_0$, where $Z_0 \sim 70\ \Omega$. This inductance is designed to resonate out the capacitive component of the diode impedance, leaving only the resistive component, which is comparable to the design impedance of the low-pass filter. This matching line also adds a series capacitive reactance of $-1.7jZ_0$ at midband for the second harmonic. This capacitive reactance largely cancels the whisker inductance at the low end of the band leading to the observed roll-off in efficiency, while at the upper end of the band this reactance decreases and the termination becomes inductive with nearly the optimal value. At much higher frequencies, the input match rapidly becomes very poor as the whisker pin resonator approaches $\lambda/4$ in length, and the efficiency drops to zero.

The frequency response of the tripler used with this receiver is shown in Fig. 8. Frequency tuning is accomplished by adjusting the input and output waveguide backshorts, with no additional tuning except to optimize the bias voltage. Backshorts are of the same contacting design as used in the mixer, and, as with the mixer, these shorts have shown excellent life. Optimum bias varies over the band; at low frequencies, the bias voltage is 2 V, with an increase to 6 V near the upper band edge. Bias current varies from zero to 5 mA depending on drive level and operating frequency. Over most of the band, maximum efficiency occurs for an input of 15–30 mW, while, for most points, the maximum safe input drive is 40–50 mW. Thus, the maximum output power is 1–4 mW from 210–250 GHz. In the rapid roll-off above 250 GHz, peak efficiency occurs for a power of up to 60 mW, and this high drive extends the useful band by 2–3 GHz.

Coincidentally the mixer's LO requirements are well matched to this tripler. Required LO power peaks at ~ 250 GHz, decreasing significantly at 195 GHz. Thus, a single tripler provides sufficient LO over the range 195–255 GHz, which includes the most useful range for the mixer.

The tripler was fitted with a scalar feed horn having an aperture limited pattern with $w_0 = 0.3$ cm, designed much like that on the mixer, except that it was equipped with a flange.

VIII. Cryogenic Image Termination

Little is known about the optimum construction or performance of absorbing materials in the 1-mm region, particularly for cryogenic use. Magnetic absorbers as used at microwave frequencies tend to be very poorly matched and so produce a high VSWR when used in simple geometries. Carbon loaded foams seem to be well matched but have very poor thermal conductivity, and are unsuitable for use in a vacuum vessel due to outgassing problems. A simple solution was found for this receiver through the use of carbon-loaded epoxy. Carbon-loaded dielectrics have a loss which increases with frequency, and a nearly saturated mixture of lamp black carbon in a 50–50 low-viscosity epoxy resin [17] produces an absorber with ~ 6-percent reflectivity at normal incidence and sufficient loss to be useful in thicknesses of only 3 mm on a metal backing. This material can readily be fabricated and its viscosity can be controlled through the exact amount of carbon added. However, its thermal conductivity, like nearly all dielectrics, is poor at low temperatures, so special care must be taken to use it in contact with a metal backing in thin layers, and with minimum room-temperature radiation falling upon it, since a room-temperature object radiates 50 mW/cm^2, enough to produce a substantial warming of this material. Also, this material tends to crack upon cooling if the rate of cooling is too great.

The cold load must work well in both polarizations since the tandem interferometer accepts both, so the design must not use polarization-dependent matching. Thus, a Brewster window as used on the mixer port is not suitable, so a simple teflon window 0.45 mm thick was used. This thickness is resonant in transmission at ~ 230 GHz and reflects less than 5 percent over an 80-GHz bandwidth. This adds, at most, 15 K to the cold load, and seems an acceptable alternative to more complex grooved or sandwich constructed windows. Teflon was chosen for the window because of its low dielectric constant and because of its

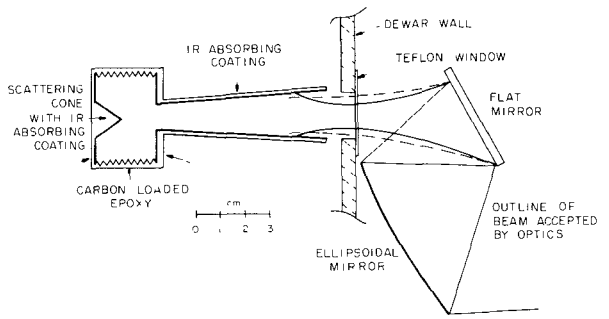

Fig. 9. Cross section through cryogenic image termination showing coupling to receiver optics.

extremely low loss, probably the lowest of any dielectric at 1 mm.

The cold-load geometry is shown in Fig. 9, as well as the two beams matching to the receiver optics. The long input taper is intended to reduce the solid angle of window (effectively emitting at 300 K) as seen by the millimeter-wave absorber. However this tube will have no effect unless its walls are absorptive in the thermal IR, because otherwise it will act as a light pipe. To accomplish this, the walls are painted with a carbon-loaded latex paint (Eccocoat SEC [12]) in a very thin layer (this paint may be thinned with water). This material shows good adhesion to metals in thin layers, even upon rapid cooling. Measurements at $\lambda \sim 10$ μm (near the peak of the thermal emission from a room-temperature black body) show ~ 90-percent absorption at 45° for a thin coating on a metal backing, while 1-mm measurements show ~ 2-percent absorption. This pipe would reduce the entering IR power of 140 mW by a factor of 300 if the walls were totally absorbing, but because a higher reflection occurs at near grazing incidence, it is likely that the actual attenuation is considerably less, and several milliwatts still remain.

The load itself consists of a cylindrical cavity with walls coated with the carbon-loaded epoxy previously described. To improve the absorption, the side walls are grooved by cutting a fine thread of 1/4 mm period 0.3 mm deep using a lathe. The end walls are ungrooved. A rough cut scattering cone is centered in the load, also coated with the IR absorbing paint, which intercepts the remaining IR entering the load, and also helps randomize the millimeter-wave reflections within the load to maintain a uniform low emissivity. Size constraints within the dewar forced this load to be quite small but it works extremely well nonetheless. A radiometric temperature of 33 K was measured at 230 GHz, and, as expected, rises to 41 K at 200 GHz and 37 K at 270 GHz. The actual internal dewar temperature is not well known, but the refrigerator used is unlikely to cool below 20–25 K given the loading upon it, so the cold load closely approaches this temperature.

IX. Dewar Geometry

The vacuum dewar consists of a simple cylinder 18 cm in diameter and 20 cm long with all cooling provided by a 1.5-W mechanical refrigerator (CTI model 21). Cold load, mixer, and IF amplifier are all mounted on a copper plate bolted to the 20-K station, while an aluminum radiation shield mounted to the 80-K station encloses all of the 20-K items. A single mechanical rotary feed-through allows backshort tuning using a drive shaft of thin-wall stainless steel tubing. All dewar parts are aluminum, which produces a high outgassing rate, but due to the low temperature within, cryopumping maintains the needed vacuum, as long as no parts ever warm up (as during a short power failure).

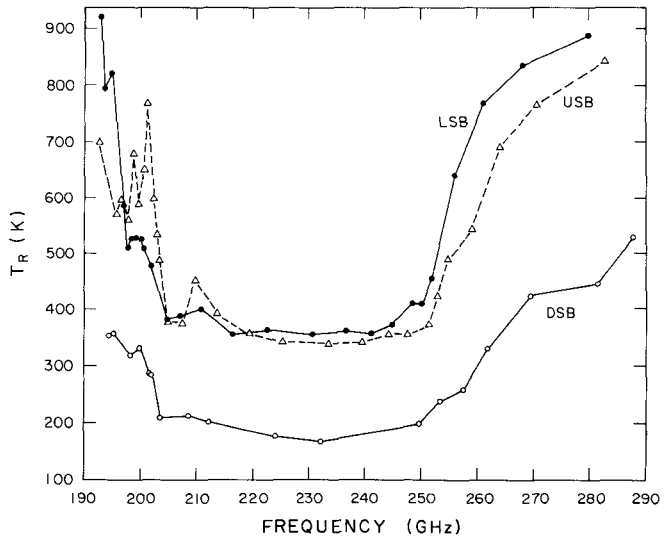

Fig. 10. Receiver noise temperatures measured for both sidebands and double sideband, at the IF center frequency of 1.4 GHz.

X. Performance

Fig. 10 shows the measured SSB and DSB performance over the full RF band, measured at the IF band center of 1.4 GHz. The receiver covers the band from 205–252 GHz with nearly flat noise while the useful band extends down to 195 GHz and up to 290 GHz. Note that while the sideband separation is only 2.8 GHz, rather substantial variations in sideband gains may occur near the band edges, and that, even over the flat portion of the band, the upper sideband is preferred. Near the lower band edge, very resonant behavior is seen in the USB performance which is not apparent in the DSB or LSB response. The cause of this is not known, but one possible source, a spurious LO klystron mode, was eliminated through tests using a second klystron which produced essentially identical results. In this frequency range, optimum dc bias voltage and backshort position vary considerably for opposite sidebands, so it is clear that the sideband impedances are very different. An advantage of a sideband filter, in this case, is that the better sideband may be selected, and that a large sideband ratio produces no calibration problems. While extensive tests have been made only with a single diode contact, previous tests have shown that the higher frequency response can be improved considerably with a shorter contact whisker, while the low end is degraded.

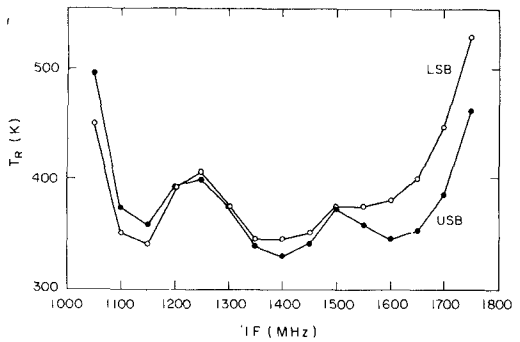

Fig. 11. SSB receiver noise temperature over the full IF band, measured with a filter bandwidth of 50 MHz, at an LO frequency of 232 GHz. Data for both sidebands is shown.

Optimum bias current is 0.2 mA with only slight variation over the full band, but optimum bias voltage due to applied LO power varies from 0.96 V at 195 GHz to 0.2 V at 250 GHz, and back to 0.9 V at 280 GHz. These widely varying LO needs seem completely uncorrelated with system noise.

Fig. 11 shows the variation in noise over the IF passband for both sidebands, measured with the LO at 232 GHz. This noise shows a ripple due to the interaction of the FET amplifier with the mixer but little other variation over 600 MHz. In USB, the lowest noise is 330 K, while the noise averaged over 550 MHz is only 360 K. Note that at the best frequency $T_{R\,\mathrm{USB}} = 330$ K, $T_{R\,\mathrm{LSB}} = 350$ K, and $T_{R\,\mathrm{DSB}} = 164$ K. The average of the two SSB measurements is 340 K, while twice the DSB noise is 328 K. If we correct the SSB results by the apparent image termination temperature of 42 K (including tandem interferometer loss), we find the average SSB temperature corrected to a 0-K image is 298 K. Thus, the combination of mixer and sideband filter shows better performance SSB than when tuned DSB. This is partly because the mixer can always be tuned to slightly improve one sideband at the expense of the other. Probably a more important reason is that the sideband filtering interferometer path difference must be doubled in order to switch from the SSB to DSB mode and this increases its diffraction loss and mode conversion.

XI. Calibration

Receiver noise measurements require black-body absorbers at two known temperatures for proper calibration, but absorbers at 230 GHz are poorly characterized. Customarily carbon-loaded foam is used as a reference at ambient temperature and after dipping in liquid nitrogen (77.3 K). In this work, a few absorbers were characterized to find the one with the lowest radiometric temperature after a liquid nitrogen dip. Eccosorb AN-72 and CV-3 [12] were measured, as well as Keene absorber AAP-4C [13]. The lowest temperature was found for the Keene material. The CV-3 has a temperature 2.5 K higher while the AN-72 is ~18 K higher.

If we assume the Keene material is truly black (it has very deep corrugations and might be expected to be very good) at 77.3 K, then the CV-3 is 79.8 K and the AN-72 is 95 K. However, we have no independent means to test this assumption and all temperatures may be somewhat higher.

All data in this paper used CV-3 as a reference with an assumed effective temperature of 80 K, except for calibration of the cold load where AN-72 was used because of its minimum thickness, which would fit into the confined space available. The Keene material is unsuitable for most tests because its effective temperature rises very quickly after removal from liquid nitrogen (~ 5 s useful time), and it is very soft and quite thick (10 cm). The CV-3 material remains cold for ~15 s, is thinner and more rigid, and thus much easier to use for lab tests.

The effective temperature is so high for AN-72 that it is unlikely to produce reliable results, but its use is sometimes necessary because it is much thinner (~1 cm) than the other choices.

XII. Receiver Noise Breakdown

The overall receiver conversion loss, from RF input to mixer IF port, is measured to be 6.2-dB SSB at room temperature, with a system noise temperature of 477 K DSB. When tuned SSB, the optics loss decreases by about 3 percent, giving an SSB receiver temperature of 908 K (if the image could be terminated at 0 K). A small additional input loss of 2 percent is due to side lobes of the feed horn. This yields a mixer conversion loss of 5.9 dB, including feed horn resistive losses. For these tests, a different IF amplifier was used, with a room temperature noise of 38 K. This yields an IF contribution of 148 K to the total. From this, we derive a mixer noise temperature of 730 K SSB.

It is useful to derive the effective diode temperature from these figures, since it is a measure of the inherent noisiness of the diode and mixer. Assuming all losses are within the mixer diode itself, this effective temperature is [18].

$$T_D = (L-2)^{-1} T_{\mathrm{MIXER}}$$
$$= 386\,\mathrm{K}.$$

In fact, input losses and the series resistance loss occur at a temperature of 295 K, so the actual value of T_D will be somewhat higher than this. This should be compared to $1/2T_{\mathrm{physical}}$ [18] for an idealized mixer, so this diode has 2.6 times the noise of an ideal mixer. Good room-temperature mixers at 100 GHz can closely approach this ideal.

The origin of this noise is not well known, but it is not unique to this diode since two other diodes of different batches and anode diameters gave comparable room-temperature results. It is likely to be due in part to the effects of the embedding circuit, contributing noise from higher harmonic terminations, and perhaps from hot-electron noise within the diode itself, due to the peak LO current inducing far more noise than in an idealized diode.

It is interesting to note that the principle difference between the noise of this mixer and the best Schottky mixer reported at 100 GHz [14] is in this effective diode temperature. In conversion loss, they are nearly the same. Thus, any significant further improvement at this frequency requires an understanding of the source of this noise.

No cryogenic measurements of conversion loss have been made, but it is likely to be about the same, with a small (~ 0.1 dB) increase expected due to the increase in R_s. A receiver noise breakdown is as follows. The measured cryogenic SSB receiver temperature is 330 K, and correcting for the effective image temperature yields 288-K SSB. Correcting for the 2-percent room-temperature loss (DSB) due to the feed side lobes gives 270 K at the input to the mixer feed horn. The IF amplifier noise temperature of ~ 10 K adds 40 K to this total. Thus, the mixer temperature is 230 K. The diode equivalent temperature, in this case, is 115 K, a factor of 3.2 lower than at room temperature, which compares with a factor of 3.7 for the best 100-GHz results [14]. This cryogenic performance is the best that has been found for several types of diodes, all giving comparable room-temperature results. However, this effective temperature is much higher than for the best 100-GHz mixer and leads to an expectation of better results when these effects are understood.

XIII. Conclusions

A Schottky diode mixer receiver has demonstrated very low-noise operation at 230 GHz over a wide RF bandwidth. True single-sideband operation is achieved with an IF bandwidth of 600 MHz. A novel optical layout helps achieve these results and a cryogenic image termination designed for a minimum effective temperature contributes only 33 K to the total. A frequency tripler generates the LO power for the receiver and provides adequate power over more than a 60-GHz tuning range.

A noise analysis shows that even lower noise should be achievable in a more ideal mixer, since the conversion loss of this mixer is only 6.0 dB, comparable to the best 100-GHz mixers, which show considerably lower noise. This rather slight frequency-dependence to the conversion loss indicates that optimized receivers at significantly higher frequency may attain comparable results.

Acknowledgment

The author would like to thank the staff of the FCRAO machine shop for their fine work on the tripler and receiver, and R. Mattauch for providing the Schottky diodes used in this receiver.

References

[1] J. W. Archer, "Millimeter wavelength frequency multipliers," *IEEE Trans. Microwave Theory Tech.*, vol. MTT-29, pp. 552–557, 1981.
[2] N. R. Erickson, "A high efficiency frequency tripler for 230 GHz," in *Proc. 12th Eur. Microwave Conf.* (Helsinki), 1982, pp. 288–292.
[3] J. W. Archer, "All solid-state low noise receivers for 210-240 GHz," *IEEE Trans. Microwave Theory Tech.*, vol. MTT-30, pp. 1247–1252, 1982.
[4] D. A. Bathker, "A stepped mode transducer using homogenous waveguides," *IEEE Trans. Microwave Theory Tech.*, vol. MTT-15, pp. 128–130, 1967.
[5] B. MacA. Thomas, "Design of corrugated conical horns," *IEEE Trans. Antennas Propagat.*, vol. AP-26, pp. 367–372, 1978.
[6] C. Dragone, "Characteristics of a broadband microwave corrugated feed: a comparison of theory and experiment," *Bell Syst. Tech. J.*, vol. 56, pp. 869–888, 1977.
[7] N. R. Erickson, "A 200–350 GHz heterodyne receiver," *IEEE Trans. Microwave Theory Tech.*, vol. MTT-29, pp. 557–561, 1981.
[8] S. Weinreb, D. L. Fenstermacher, and R. Harris, "Ultra low-noise 1.2–1.7 GHz cooled GaAsFET amplifiers," *IEEE Trans. Microwave Theory Tech.*, vol. MTT-30, pp. 849–853, 1982.
[9] N. R. Erickson, "Off-axis mirrors made using a conventional milling machine," *Appl. Opt.*, vol. 18, pp. 956–957, 1979.
[10] N. R. Erickson, "A directional filter diplexer using optical techniques for millimeter to submillimeter wavelengths," *IEEE Trans. Microwave Theory Tech.*, vol. MTT-25, pp. 865–866, 1977.
[11] P. F. Goldsmith, "Quasioptical techniques at millimeter and submillimeter wavelengths," in *Infrared and Millimeter Waves*, vol. 6, K. J. Button, Ed. New York: Academic, 1982.
[12] Emerson and Cuming, Canton, MA.
[13] Keene Microwave, Advanced Absorber Products, Amesbury, MA.
[14] C. R. Predmore, A. V. Raisanen, N. R. Erickson, P. F. Goldsmith, and J. L. R. Marrero, "A broad-band, ultra-low-noise Schottky diode mixer receiver from 80 to 115 GHz," *IEEE Trans. Microwave Theory Tech.*, vol. MTT-32, pp. 498–507, 1984.
[15] H. Kogelnik and T. Li, "Laser beams and resonators," *Appl. Opt.*, vol. 5, pp. 1550–1567, 1966.
[16] Corning Glass Works, Corning, NY.
[17] Chemlok 305, Hughson Chemicals, Erie, PA.
[18] A. R. Kerr, "Shot-noise in resistive-diode mixers and the attenuator noise model," *IEEE Trans. Microwave Theory Tech.*, vol. MTT-27, pp. 135–140, 1979.

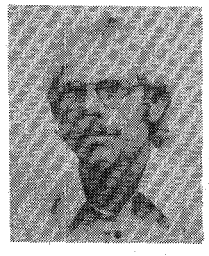

Neal R. Erickson (M'85) was born in Peoria, IL, on January 3, 1949. He received the B.S. degree from the California Institute of Technology, Pasadena, in 1970, and the Ph.D. degree from the University of California, Berkeley, in 1979.

Since 1979, he has been working as a Post-Doctoral Associate at the Five College Radio Astronomy Observatory, University of Massachusetts, Amherst. He is involved in the development of receivers, quasi-optical devices, and frequency multipliers for the near-millimeter and submillimeter regions, and is also active in the field of millimeter and submillimeter radio astronomy.